Volume 20 | Number 18 | 21 September 2018 | Pages 4123–4380

Green Chemistry

Cutting-edge research for a greener sustainable future

rsc.li/greenchem

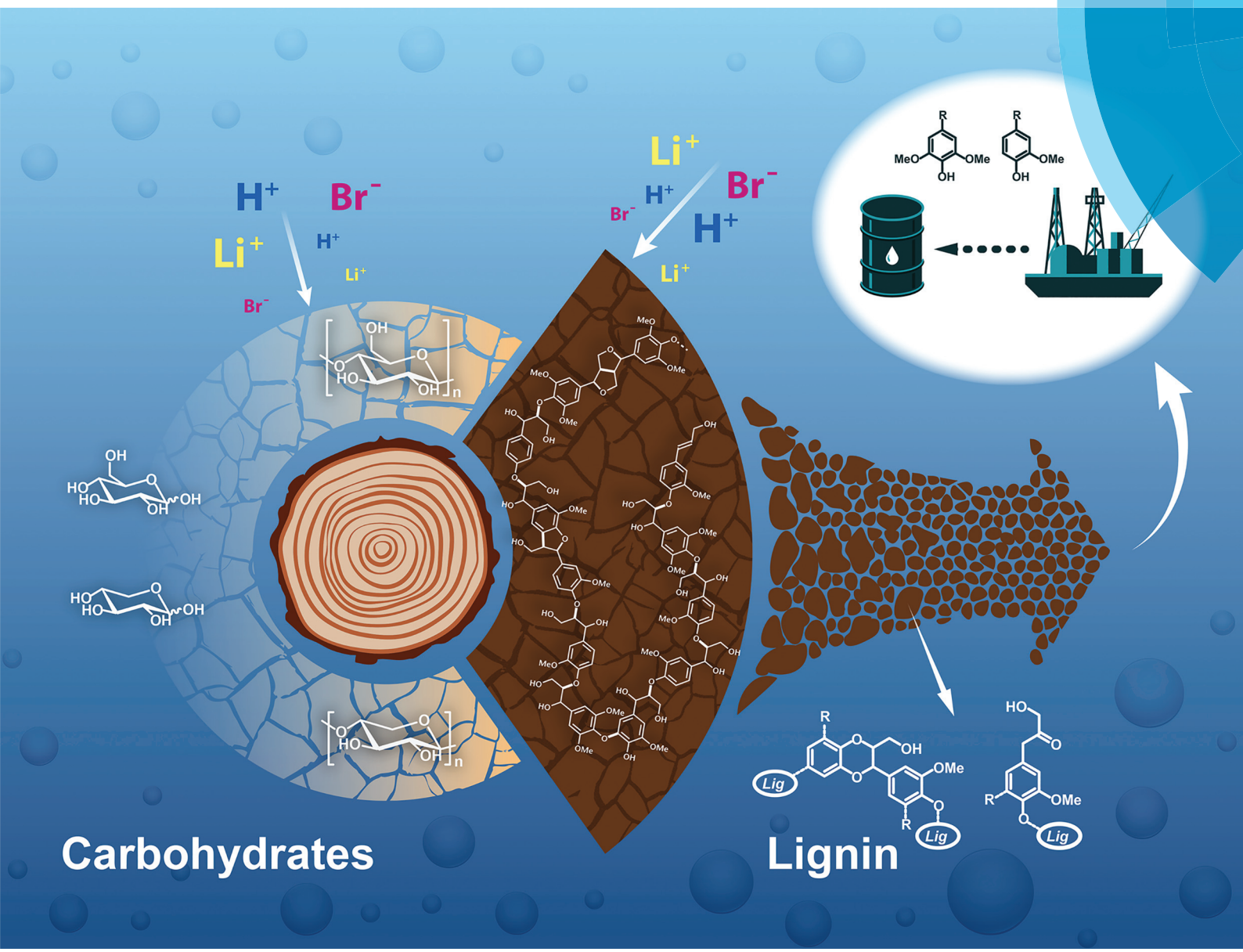

ISSN 1463-9262

ROYAL SOCIETY OF CHEMISTRY

PAPER

Xuejun Pan *et al.*

An uncondensed lignin depolymerized in the solid state and isolated from lignocellulosic biomass: a mechanistic study

Green Chemistry

PAPER

View Article Online
View Journal | View Issue

Cite this: *Green Chem.*, 2018, **20**, 4224

An uncondensed lignin depolymerized in the solid state and isolated from lignocellulosic biomass: a mechanistic study†

Ning Li, [a] Yanding Li, [a,b] Chang Geun Yoo, [a,c] Xiaohui Yang,[a,d] Xuliang Lin,[a,e] John Ralph [a,b] and Xuejun Pan *[a]

This study demonstrated that lignin could be efficiently depolymerized in the solid state with minimal condensation and separated from biomass with high purity by dissolving and hydrolyzing cellulose and hemicelluloses, using an acidic lithium bromide trihydrate (ALBTH) system under mild conditions (with 40 mM HCl at 110 °C). The ALBTH lignins isolated from biomass sources representing the three plant classes (hardwoods, softwoods, and grasses) contained abundant uncondensed moieties (*i.e.*, Hibbert's ketones and benzodioxanes). The benzodioxane structure was identified and confirmed for the first time in an acid-depolymerized lignin. Reactions using lignin model compounds (LMCs, guaiacylglycerol-β-guaiacyl ether and various aromatic monomers) confirmed the formation of the uncondensed moieties and revealed the synergy between LiBr and acid in inducing the crucial intermediate benzyl carbocations, which then led to cleavage of the β-*O*-4-aryl ether bonds to produce Hibbert's ketones, demethylation to produce benzodioxanes, and condensation reactions. Unlike in the LMC reactions, the condensation of the real lignin in biomass under ALBTH conditions was greatly diminished, possibly due to lignin remaining in the solid state, limiting its mobility and accessibility of the benzyl carbocation to the electron-rich aromatic sites for condensation. Preliminary results indicated that, because of its uncondensed nature, the ALBTH lignin was a good lignin feedstock for hydrogenolysis. This study provided a new approach to effectively isolate depolymerized lignin from lignocellulose in a less condensed form for boosting its downstream valorization.

Received 24th March 2018,
Accepted 5th June 2018

DOI: 10.1039/c8gc00953h

rsc.li/greenchem

1. Introduction

Lignin, as a major cell wall component of lignocellulosic biomass, is the most abundant aromatic biopolymer on the Earth. Lignin valorization has emerged as a consensus requirement for profitability, based on efficiently utilizing the entire lignocellulosic biomass. In view of the structural and functional nature of lignin, a broad array of potential applications is anticipated, including as dispersants, aromatic platform chemicals, fuel precursors, pharmaceutical products and ingredients for adhesives, resins, biocomposites, and carbon fibers.[1–5] In efforts to separate lignin from lignocellulose and achieve value-added utilization, chemocatalytic depolymerization of lignin by cleaving the inter-unit ether linkages (mostly β-*O*-4-aryl ether bonds) but avoiding condensation (repolymerization) reactions is recognized to be a prerequisite.

Acid is prevalently used for lignin depolymerization, cleaving β-*O*-4-aryl ether bonds initiated by an α- (or benzyl) carbocation intermediate. Acid-catalyzed lignin depolymerization has been extensively studied in many solvent systems, including ionic liquids[6–8] and various organic solvents such as γ-valerolactone,[9] dioxane,[10–14] methanol,[15] ethanol,[16,17] formic acid,[18] and acetic acid.[19,20] However, acid-catalyzed lignin depolymerization is always accompanied by condensation reactions that take place either before or after the cleavage of the β-ether units. Before cleaving the β-*O*-4-aryl ether bond, the benzyl carbocation can attack an electron-rich aromatic ring in an electrophilic aromatic substitution reaction, leading to formation of a new C–C linkage that defines con-

[a]*Department of Biological Systems Engineering, University of Wisconsin-Madison, Madison, WI, 53706, USA. E-mail: xpan@wisc.edu; Fax: +1-608-2621228; Tel: +1-608-2624951*
[b]*Department of Biochemistry, University of Wisconsin-Madison, WI, 53706, USA*
[c]*BioEnergy Science Center and Bioscience Division, Oak Ridge National Laboratory, Oak Ridge, TN 37831, USA*
[d]*Institute of Chemical Industry of Forestry Products, Chinese Academy of Forestry, Nanjing 210042, China*
[e]*School of Chemical Engineering and Light Industry, Guangdong University of Technology, Guangzhou, 511400, China*
†Electronic supplementary information (ESI) available. See DOI: 10.1039/c8gc00953h

densation.[21–23] After the cleavage of the β-*O*-4-aryl ether bond, the resulting C2-aldehyde (a phenylacetaldehyde fragment) and Hibbert's ketone (**HK**) end-groups are vulnerable to aldol condensation under acidic conditions, forming other inert C–C linkages.[10,24] Previous studies have explored different means of avoiding or reducing the condensation reactions by introducing trapping/capturing reagents or pretreatment by, for example, trapping the benzyl carbocation using aromatic compounds such as phenol,[22,23] protecting the α-carbon from condensation by forming a 1,3-dioxane structure with the α- and γ-hydroxyls of lignin using formaldehyde[12] or other aldehydes,[25] or *in situ* capturing of the unstable post-cleavage carbonyls, *e.g.*, the C2-aldehyde and **HK**, by producing acetals using diols such as ethylene glycol.[10,11,15]

Intrinsically, the success of lignin depolymerization to produce uncondensed lignin relies on the competition between ether cleavage and condensation. As the occurrence of condensation requires two adjacent lignin moieties or species (*i.e.*, between the benzyl carbocation and the electron-rich aromatic ring, or between the C2-aldehydes and/or **HK**s), preventing the lignin moieties from direct contact can block or reduce condensation. Therefore, it is hypothesized that lignin condensation could be avoided or minimized by limiting the accessibility or mobility of the reactive lignin moieties (intermediates) by, *e.g.*, keeping lignin in the solid state during the acid-catalyzed depolymerization (the cleavage of the β-*O*-4-aryl ether bond), and using mild conditions (low acid concentration and moderate temperature) such as in the LiBr system described below.

According to our previous studies, the acidic lithium bromide trihydrate (ALBTH, $LiBr{\cdot}3H_2O$) system exhibited an extraordinary ability to swell, dissolve, and hydrolyze polysaccharides (cellulose and hemicelluloses) in lignocellulose.[26,27] The lignin fraction (ALBTH lignin) could be quantitatively obtained as the insoluble residue remaining after hydrolyzing the carbohydrates.[28] It was found to have a low molecular weight and was highly soluble in many common organic solvents, such as THF, acetone, acetic acid/water (95/5, v/v), dioxane/water (9 : 1, v/v), and DMSO (unpublished data). This feature distinguishes it from other isolated lignins such as Klason lignin and kraft lignin and indicates the uniqueness of lignin depolymerization in the ALBTH system. In addition, when the technical lignins from different pulping and biorefining processes were treated in the ALBTH system under mild conditions, the cleavage of the aryl ether bonds was also observed, leading to further reductions in molecular weight.[29] It is therefore of significant interest to investigate the chemical changes of lignins in the ALBTH system, to provide new insights into the lignin depolymerization mechanisms and to determine the characteristics and potential utilization of the ALBTH lignin. In this study, the native lignin in different lignocellulosic feedstocks and lignin model compounds (LMCs) were utilized to elucidate the mechanisms and pathways of lignin depolymerization and condensation in the ALBTH system.

2. Experimental section

2.1 Chemicals

Chips of hardwood (aspen, poplar and eucalyptus) and softwood (Douglas fir), and coarsely chopped grasses (switchgrass and corn stover) were ground with a Wiley-mill, and the fraction between 20 and 100 mesh was collected as lignocellulosic materials for this study. Chemicals including 3,4,5-trimethoxylbenzyl alcohol (**TMBA**), guaiacol (**GA**), creosol (**CS**), anhydrous lithium bromide (LiBr), hydrochloric acid (HCl), dimethylsulfoxide (DMSO-d_6), pyridine-d_5, pyridine, tetrahydrofuran (THF), acetonitrile, and *N*-methyl-*N*-trimethylsilyltrifluoroacetamide (MSTFA) were purchased from Fisher Scientific (Pittsburgh, PA), VWR (Radnor, PA), and Sigma Aldrich (St Louis, MO). Guaiacylglycerol-β-guaiacyl ether (**GG**) was synthesized and provided by Dr Gaojin Lyu with ~99% purity, as determined by NMR.[30]

2.2 Isolation of the ALBTH lignin fraction from biomass

The ground biomass was mixed with the ALBTH solution (60 wt% LiBr containing 40 mM HCl) at room temperature in a 40 mL glass vial fitted with a Teflon-lined screw cap; a magnetic stir-bar was added. The mixture in the vial was heated in an oil bath at 110 °C with magnetic stirring (400 rpm) to hydrolyze cellulose and hemicelluloses to soluble fractions. After the preset reaction time, the reaction was quenched by placing the vial into an ice-water bath. The insoluble ALBTH lignin fraction was collected by vacuum filtration on a filtering crucible and thoroughly washed with deionized (DI) water. The solid sample was dried at 50 °C under vacuum for subsequent analyses.

2.3 Reactions of lignin model compounds (LMCs) in ALBTH

Various aromatic monomers and dimers (including **GA**, **CS**, **TMBA**, and **GG**) were used as LMCs to investigate the reaction mechanism in the lithium bromide trihydrate (60 wt%) medium with or without an acid catalyst. A dilute acid solution (10 mM HCl) in the absence of LiBr was used as the control. Due to the limited solubility of LMCs in 60% LiBr at room temperature, LMCs (individually or in pairs) were first dissolved in dioxane prior to mixing with ALBTH (the final ratio of dioxane to ALBTH was ~5/95, v/v). The mixture was then sonicated for 5 min to obtain a homogeneous suspension of LMCs in ALBTH. During subsequent heating, the suspension became a transparent solution. The reaction was conducted following the same procedure as for the biomass above but with reduced reaction severity (temperature: 100 °C and acid concentration: 10 mM HCl). During the reaction, aliquots were taken for analysis at preset intervals. After the reaction, the mixture was extracted triply with CH_2Cl_2 to recover products. The CH_2Cl_2 phase was washed with water to remove the salts. The aqueous phase was filtered to collect the insoluble products (especially from the **GG** reactions). The insoluble products were washed with DI-water and dissolved in acetone. The products in CH_2Cl_2 and acetone were combined, dried over anhydrous Na_2SO_4, and the solvents were removed by rotary

evaporation at reduced pressure. Samples were stored at −4 °C for subsequent analyses.

2.4 Acetylation of ALBTH lignin

Lignin (0.1 g) was dispersed/dissolved in 1 mL pyridine in a 20 mL glass vial, and then acetic anhydride (1 mL) was added. The mixture was sealed and allowed to react at room temperature for 72 h. Lignin acetate was precipitated in acidic water (pH < 2) with constant stirring, collected by filtration, washed with DI-water, and vacuum-dried.

2.5 NMR spectroscopic analysis

Nuclear magnetic resonance (NMR) spectra were recorded on a Bruker AVANCE III 500 MHz spectrometer equipped with a DCH (^{13}C-optimized) cryoprobe (Billerica, MA). The lignin and GG reaction samples (unacetylated) were dissolved in 0.5 mL of dimethylsulfoxide-d_6 (DMSO-d_6) or DMSO-d_6/pyridine-d_5 (4 : 1, v/v). Heteronuclear single-quantum coherence (HSQC) spectra were recorded at 25 °C using Bruker's standard hsqcetgpsisp2.2 pulse program (acquisition times 200 ms and 8 ms in ^{1}H and ^{13}C dimensions, respectively; inter-scan relaxation delay 1 s). HSQC-total correlation spectroscopy (TOCSY) spectra were recorded at 25 °C using Bruker's standard hsqcdietgpsispp2 pulse program (inter-scan relaxation delay 2 s; mixing time 80 ms). Data processing was performed using Bruker's Topspin 3.5 software to a final matrix size of 2k × 1k data points.

The relative abundance of each interunit linkage R_i, appearing in the aliphatic region of the HSQC spectra, from lignin samples was calculated using the following equation:

$$R_i\% = I_i/[I_A + I_B + I_C + I_{HK} + I_{BD}] \times 100\%$$

where I_i, I_A, I_B, I_C, I_{HK}, and I_{BD} denote the α-H/C correlation peak integrals of the target inter-unit linkage **i**, β-*O*-4-aryl ether **A**, phenylcoumaran (β-5) **B**, resinol (β-β) **C**, **HK**, and benzodioxane **BD** structures; **HK** and **C** units have two α-protons per unit, so their integrals are halved in the relative abundance calculation.

2.6 Gel-permeation chromatographic (GPC) analysis

The number-average and weight-average molecular weights (M_n and M_w, respectively) of the ALBTH lignins (after acetylation) and the products of LMCs were estimated on a Dionex ICS-3000 system equipped with three tandem 300 mm × 7.8 mm (L. × I.D.) Phenogel 5U columns (10 000, 500, and 50 Å, respectively) and a 50 mm × 7.8 mm (L. × I.D.) Phenogel 5U guard column (Phenomenex, Torrance, CA). The eluent was an isocratic 100% THF (HPLC grade without a stabilizer) at a flow rate of 1.0 mL min^{-1} and the column temperature was maintained at 30 °C. Each sample (~0.5%) in THF was injected after passing through a 0.45 μm filter and the fractionated lignin in the column eluent was detected using a variable wavelength detector (VWD) at 280 nm. The apparent molecular weight was calibrated using polystyrene standards and **GG** at 254 nm.

2.7 Gas chromatography-mass spectrometric (GC-MS) analysis

Qualitative analysis of the LMC reaction products was conducted on a GC-MS system (GCMS-QP 2010S, Shimadzu Co., Addison, IL) with an SHRXI-5MS column (30 m × 0.25 mm, L. × I.D., with 0.25 μm film thickness). The injection port was at 280 °C, and the carrier gas was helium at a flow rate of 8 mL min^{-1} in a split mode (split ratio, 5 : 1). The programmed GC oven temperature profile started with a 30 °C isotherm for 5 min, followed by a 5 °C min^{-1} ramping to 220 °C and subsequent 10 °C min^{-1} ramping to 300 °C, then held at the temperature for 5 min. The products from the **GG** reaction were silylated to improve the sample volatility. Specifically, an approximately 50 μL sample was mixed and reacted with a 500 μL *N*-methyl-*N*-trimethylsilyl-trifluoroacetamide (MSTFA)/pyridine mixture (1 : 1, v/v) at room temperature for 2 h.

2.8 High-performance liquid chromatographic (HPLC) analysis

The LMC reaction products were quantitated on a Dionex ICS-3000 system equipped with a YMC-Triart C18 column (250 mm × 4.6 mm, L. × I.D.) at 30 °C and a VWD set at 210 nm. Both samples and standards were diluted with 20% acetonitrile in water to ensure full dissolution and filtered through a 0.45 μm syringe filter prior to injection. The mobile phase was an isocratic acetonitrile/water solution (20/80, v/v) with addition of 0.1% phosphoric acid at 0.8 mL min^{-1}. The column was reconditioned using an isocratic acetonitrile/water solution (60/40, v/v) for 10 min after each run.

3. Results and discussion

3.1 Formation of HK and BD moieties from lignin depolymerization in the ALBTH system

Feedstocks (aspen, poplar, eucalyptus, Douglas fir, switchgrass, and corn stover) representing the three major biomass classes (hardwoods, softwoods, and grasses) were treated in the ALBTH system under mild reaction conditions (110 °C, LiBr 60 wt% and 40 mM HCl) to investigate lignin depolymerization in the process of ALBTH treatment. By completely dissolving and hydrolyzing cellulose and hemicelluloses, the ALBTH treatment allowed quantitative isolation of lignin in the solid state from biomass,[28] as shown in Table S1.† The GPC-estimated molecular weights of the lignins are listed in Table 1 and compared with those of the corresponding isolated lignins, such as milled wood lignin (MWL) and cellulolytic enzyme lignin (CEL), estimated under similar chromatographic conditions.[31–34] MWL and CEL fractions are generally considered to incur only minor modifications to the native lignin and therefore acceptable to represent the native lignin in the biomass. However, the molecular weights of MWL and CEL are slightly lower than that assumed for native lignin, because they only represent the solvent-extractable (low molecular weight) portions of the native lignin.

Table 1 Average molecular weights and polydispersity indices of the representative isolated lignins and ALBTH lignins from various biomass

Biomass	Treatment	M_n	M_w	PDI
Poplar	MWL[31]	4100	10 000	2.4
	ALBTH-30 min	1200	2900	2.5
	ALBTH-120 min	1100	3200	2.9
Aspen	MWL[32]	4500	23 300	5.2
	ALBTH-30 min	1000	2200	2.2
Eucalyptus	CEL[33]	5500	17 200	3.1
	ALBTH-120 min	1100	2500	2.2
Douglas fir	CEL[33]	5500	21 800	4.0
	ALBTH-30 min	1100	3700	3.3
	ALBTH-120 min	1100	3600	3.3
Corn stover	CEL[34]	1400	10 100	7.4
	ALBTH-30 min	1200	4100	3.3
Switchgrass	MWL[33]	2100	5100	2.5
	ALBTH-120 min	1000	3100	3.1

The molecular weights of all the lignin samples (both in this study and in the literature) were estimated after acetylation (with either acetic anhydride or acetyl bromide) using gel-permeation chromatography (GPC) under similar conditions (a UV detector, THF as the eluent, and polystyrene as the standards for calibration).

The weight-average molecular weight (M_w) dropped to below 3000 Da for the hardwood (aspen, poplar, and eucalyptus) ALBTH lignins and 3700 Da for the softwood (Douglas fir), after treatment in ALBTH for 30 min. These M_w values are markedly lower than those of isolated lignins (CEL and MWL, 10K–25K Da). The results suggest that the native lignin in woody biomass was extensively depolymerized in the ALBTH system. Extending the ALBTH treatment to 120 min, the M_w of the lignins did not decrease further, suggesting that the cleavage of the β-*O*-4-aryl ether bonds was less prevalent and/or that lignin condensation was occurring, as discussed below. Similarly, the native lignin in grassy biomass such as corn stover and switchgrass was depolymerized to low molecular weight polymers (M_w 3100–4100 Da) in the ALBTH system.

To reveal the structural changes in lignin during the depolymerization, the ALBTH lignins from aspen, eucalyptus, Douglas fir, and corn stover were characterized using HSQC NMR. Their spectra were compared with those from the whole cell wall (WCW) of the corresponding raw biomass, as shown in Fig. 1 (the aliphatic region) and Fig. S1† (the aromatic region). Many of the major contours in the δ_C/δ_H 65–85/2.5–4.5 ppm region of the WCW spectra (left column) assigned to the non-anomeric carbohydrates are mostly absent in the ALBTH lignin spectra (right column), verifying the excellent ability of ALBTH to dissolve and hydrolyze the carbohydrates from the biomass to leave a relatively pure lignin fraction. As shown in Fig. 1A, C, E, and G (left column), the native biomass lignins had abundant β-ether units **A** (with their characteristic β-*O*-4-aryl ether linkages) along with small amounts of phenylcoumarans **B** (β-5) and resinols **C** (β-β), which are in agreement with other studies.[35,36] After a mild ALBTH treatment, the signals from the β-ether units were attenuated and some new chemical structures including the **HK** and **BD** moieties were revealed. The assignment of the Hibbert's ketone moiety **HK** was made by the cross peaks at δ_C/δ_H 44.5/3.67 ppm (α-position) and 67.1/4.19 ppm (γ-position) according to the study on LMCs,[13] and the assignment of the *trans*-benzodioxane moiety **BD** was made by the cross peaks at δ_C/δ_H 75.6/4.86 ppm (α-position) and 77.5/4.07 ppm (β-position) according to the study on **C**-lignin and **C**-DHP polymers derived from caffeyl alcohol polymerization.[37] Notably the resonance peaks from both moieties were distinctive from other lignin signals and were consistently observed in the ALBTH lignins from all woody biomass species used in this study. The ALBTH lignin from grasses (corn stover, Fig. 1H) only had **HK**, but not **BD** moieties resolved, possibly due to its low β-*O*-4-aryl ether content and the presence of *p*-coumarates and ferulates. The identification of **HK** and **BD** moieties suggests that the condensation to form the inert C–C linkages was less significant (or reduced) during the cleavage of the β-*O*-4-aryl ether bonds in ALBTH. More evidence and discussion will be provided below from the LMC study. A striking feature of the reaction was the generation of **BD** units, obviously from β-ether units and involving demethylation. As far as we are aware, this is the first time that **BD** units have been detected from an acid-catalyzed lignin depolymerization. **BD** units were originally discovered in vanilla seed coats that make their lignins entirely from caffeyl alcohol,[37] with its "**C**-lignin" being recently positioned as an ideal lignin structure that can survive acidic treatments but can be readily depolymerized to valuable 4-propanolcatechol and its derivatives.[38,39] These observations suggest that the ALBTH system has the uniqueness to yield uncondensed and valuable lignin moieties/structures, compared with other acidic solvent systems for lignin depolymerization. The presence of **G**, **S**, and **H** units in lignin before/after ALBTH treatment is most readily discerned from the aromatic regions of the HSQC spectra and can be verified with reference to Fig. S1.† Notably, the formation of **HK** and **BD** moieties significantly changed the chemical shifts of **G** and **S** units in the aromatic regions.

Using semi-quantitative analysis, the relative abundance of various units in the lignins was estimated, as shown in Table 2. The phenylpropanoid units in hardwood species such as aspen were mainly the β-*O*-4-aryl ether **A** and resinol **C** moieties with a trace amount of the phenylcoumaran **B** moiety. After ALBTH treatment, the relative abundance of the resinol **C** moiety remained unchanged, while the β-ether **A** decreased from 91% to 25% and phenylcoumaran **B** was no longer detectable. Notably, **HK** and **BD** (as novel uncondensed lignin depolymerization products) formed in 46% and 23% levels, respectively. For softwood species (*e.g.*, Douglas fir), the relative level of resinol **C** rose from 4% to 8%, whereas the β-ether **A** and phenylcoumaran **B** moieties decreased from 79% and 18% to 13% and 18%, respectively. These results suggested that the ease of cleaving the lignin linkages during the ALBTH treatment followed the order of β-ether > phenylcoumaran > resinol (*i.e.*, **A** > **B** > **C**). In other words, the ALBTH system was able to cleave the β-ether **A** in lignin fairly selectively, leading to uncondensed **HK** and **BD** moieties. Notably, it was observed that the hardwood lignin had a much higher

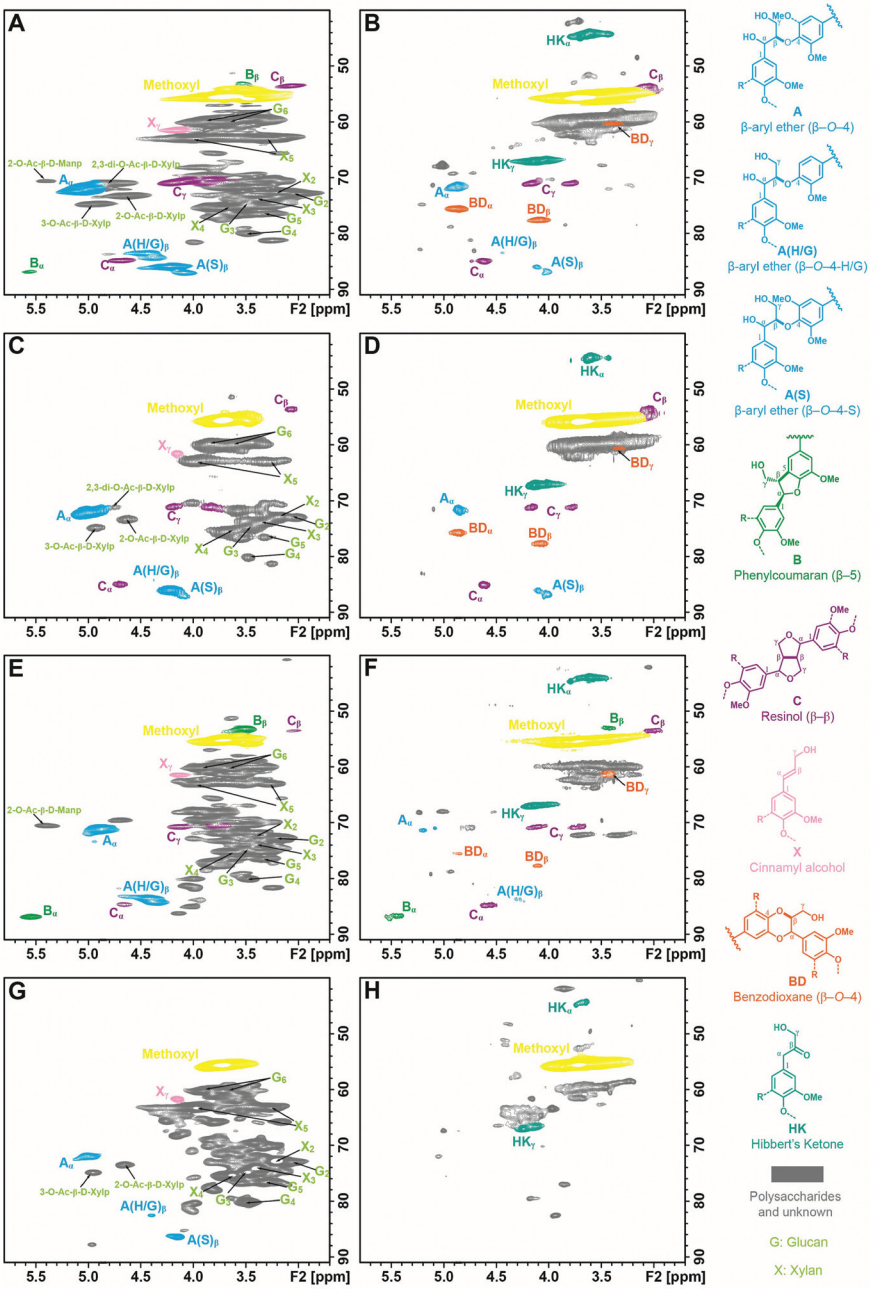

Fig. 1 The aliphatic regions of 2D $^{1}H-^{13}C$ correlation (HSQC) spectra of the ball-milled plant cell walls dispersed in DMSO-d_6/pyridine-d_5 (A: aspen, C: eucalyptus, E: Douglas fir, and G: corn stover) and the lignins isolated by acidic lithium bromide trihydrate treatment in DMSO-d_6 (D: eucalyptus and F: Douglas fir) and in DMSO-d_6/pyridine-d_5 (B: aspen and H: corn stover). Correlation signals are categorized and color-coded by the type of aromatic units. (**A**, β-*O*-4-aryl ether; **B**, phenylcoumaran (β-5); **C**, resinol (β-β); **X**, cinnamyl alcohol end-group; **HK**, Hibbert's ketone; and **BD**, benzodioxane).

level of the **BD** moiety (over 23%) than the softwood lignin (5%) after the ALBTH treatment. Apparently, the **S** type lignin (abundant in hardwood) has more chances to demethylate one of the two methoxyl groups to form a **BD** moiety than the **G** type lignin in softwood that has only one methoxyl group per unit.

As mentioned above, the acid-catalyzed lignin depolymerization has been extensively studied in the systems such as acidic ionic liquid,[6] aqueous dilute acid,[40] steam explosion,[41] and in acidic organic solvents such as methanol, GVL, and dioxane.[9,11,13] However, the **HK** from cleavage of the β-ether units was not observed or barely visible in the HSQC NMR spectra of the lignins from these processes. There are presumably two reasons. First, the competing C6–C2 type cleavage might be more favorable than the C6–C3 type cleavage in the traditional acid systems (especially in H_2SO_4-catalyzed

Table 2 Relative abundance of the major inter-unit linkages in the native and ALBTH lignins by the semi-quantitative HSQC NMR analysis

Lignin unit		C	B	A	HK	BD
Aspen	WCW	6.3	2.6	91.1		
	ALBTH	5.2		25.3	46.3	23.1
Eucalyptus	WCW	5.0		95.0		
	ALBTH	9.8		31.0	33.6	25.6
D. fir	WCW	3.6	17.5	78.9		
	ALBTH	7.8	17.9	13.2	56.1	5.0

systems), resulting in abundant C2-aldehyde end-groups that promptly succumb to aldol condensations.[10,42–44] This was supported by the finding that the cleavage pathways were dependent on the types of acid and solvent systems used.[45] Second, the **HK** (C3 type ketone) end-groups might be preferentially stabilized or prevented from condensation in the ALBTH system because, in the solid state, the lignin moiety was less accessible and less mobile, limiting the opportunity for condensation reactions, as further discussed below. In summary, the observations above suggest that the ALBTH system is able to selectively cleave the β-*O*-4-aryl ether bonds under mild reaction conditions and generate depolymerized and less condensed lignins containing novel **HK** and **BD** moieties. Compared with other acidic systems, the ALBTH system showed considerable potential to isolate "good" lignin from lignocellulosic biomass for valorization.

3.2 Reactions of LMCs in ALBTH

Guaiacylglycerol-β-guaiacyl ether (**GG**), a popular β-*O*-4-aryl ether model compound, was used to investigate lignin depolymerization in ALBTH. The decomposition of **GG** and the yield of guaiacol (**GA**) are presented as a function of the reaction time in Fig. 2. **GG** and **GA** were quantitated by HPLC (Fig. S2†). In order to investigate the possible synergy of LiBr and acid in ALBTH, the **GG** reaction was conducted at 100 °C in three disparate solvent systems: acidic lithium bromide trihydrate (ALBTH) with 10 mM HCl, neutral lithium bromide trihydrate (NLBTH) without acid, and an aqueous dilute acid (DA) solution with 10 mM HCl but without LiBr. In ALBTH (Fig. 2A), **GG** was completely consumed within 10 min, yielding 34% **GA**; extending the reaction, no additional **GA** was released. Without an acid catalyst, the conversion of **GG** was slow in NLBTH (Fig. 2B). The **GG** content (both the *erythro* and *threo* diastereomers) gradually decreased with time, and over 80% conversion was reached at 180 min. In this case, the *erythro*-isomer was depleted more rapidly, as has been previously observed under alkaline degradation conditions.[46] However, the yield of **GA** was negligible (less than 2%). This observation indicated that most **GG** was slowly transformed in NLBTH, but no **GA** was released, possibly because either the β-*O*-4-aryl ether bonds were not cleaved, or the released **GA** promptly condensed with **GG** decomposition products. The analysis results of **GG** condensation products in NLBTH mentioned later apparently support the fact that the former was the primary reason. The results shown in Fig. 2B also verified that the presence of acid was essential to the effective cleavage of the β-ether. However, acid alone (10 mM HCl in water) without LiBr did not break down **GG** at 100 °C (Fig. 2C). The total **GG** content in the system remained without apparent change over 3 h and without formation of **GA**, although *threo*-**GG** partially isomerized to *erythro*-**GG**, resulting in the apparent equilibrium favoring the *erythro*-isomer. Notably, higher reaction temperatures and higher acid concentrations (*e.g.*, 150 °C with 200 mM H_2SO_4) were usually necessary to catalyze the cleavage of **GG** in the aqueous dilute acid.[40] The observation of the effective cleavage of **GG** under milder conditions (very low acid concentration and moderate temperature, 10 mM HCl and 100 °C) in lithium bromide trihydrate was presumably ascribed to (1) the synergy between the acid and LiBr in cleaving the β-*O*-4-aryl ether bond, and (2) the enhanced acidity of the Brønsted acid in LiBr trihydrate.[47] The aforementioned results demonstrated that both acid and LiBr trihydrate synergistically depolymerized lignin in the ALBTH system under mild conditions. A similar synergistic effect of the acid and LiBr trihydrate in ALBTH was reported in the hydrolysis and dehydration of polysaccharides to furfurals.[47,48]

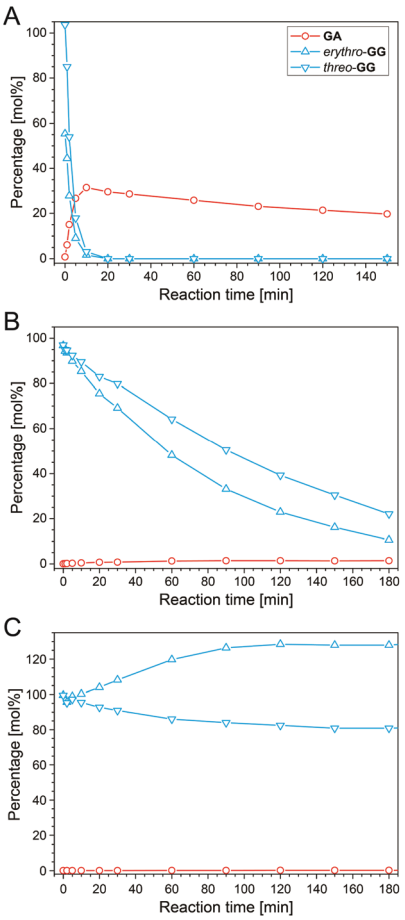

Fig. 2 Reactions of guaiacylglycerol-β-guaiacyl ether (**GG**) in acidic lithium bromide trihydrate (A), neutral lithium bromide trihydrate without acid (B), and acidic water solution (C). Reaction conditions: 100 °C, 1 g L^{-1} **GG** dimer concentration, and 10 mM HCl for A and C.

The structures of the **GG** products in ALBTH and NLBTH were further characterized by HSQC NMR analysis. **HK** and **BD** moieties were detected from the ALBTH-treated **GG** (Fig. 3A), whereas only a negligible amount of **HK** but no **BD** was identified from the NLBTH-treated **GG** (Fig. 3B). **HK** was also detected in the HPLC analysis of **GG** treated in both ALBTH and NLBTH (Fig. S2†). The formation of **HK** and **BD** was further confirmed by the GC-MS analysis (Fig. S3B†) of the ALBTH-treated **GG**, in which a **HK** monomer and 4-(3-(hydroxymethyl)-2,3-dihydrobenzo-[*b*][1,4]dioxin-2-yl)-2-methoxyphenol (a **BD** dimer) were detected. These verified our previous observation that both **HK** and **BD** moieties are formed during lignin depolymerization in ALBTH. No **BD** was identified in NLBTH-treated **GG**, suggesting that acid was crucial to generate the uncondensed **BD** structures in the LiBr trihydrate system. The relatively low abundance of the **BD** moieties from **GG** was consistent with our biomass HSQC NMR results above, in which **G** units (softwood lignin) were less prone to form the **BD** structures than **S** units (hardwood lignin).

Condensation products from **GG** were also detected in the HPLC analysis (Fig. S2†) and further confirmed by GPC analysis (Fig. S4†). Both ALBTH and NLBTH systems yielded higher molecular weight fractions from **GG**. As shown in Fig. S4,† the sample from the ALBTH system had a broad peak A (M_w: 750 Da, M_n: 630 Da) and a sharp peak B (M_w: 290 Da, M_n: 290 Da) with the A to B intensity ratio (A/B) = 2.1. For the sample from the NLBTH system, the peaks A and B represented the M_w/M_n of 780/660 and 290/280, respectively, with A/B = 4.3. These results indicate that the products from the NLBTH-treated **GG** had more condensed structures and slightly higher molecular weights than that from the ALBTH-treated **GG**. This is in agreement with the results shown in Fig. 2B where **GG** was consumed but did not release **GA**, implying that condensation was predominant over cleavage of the β-*O*-4-aryl ether bond in NLBTH.

The structures of the condensation products from **GG** were identified by HSQC NMR (Fig. 3) in which the assignments were made based on the GC-MS results shown in Fig. S3† and HSQC-TOCSY NMR results shown in Fig. S5.† In the ALBTH-treated **GG** sample, the diphenylmethane-type condensation products were unveiled, including the 4-(3-hydroxy-1-(3-hydroxy-4-methoxyphenyl)-2-(2-methoxyphenoxy) propyl)-2-methoxyphenol trimer (**CD-I** type condensation) and the 3-(4-hydroxy-3-methoxyphenyl)-3-(3-hydroxy-4-methoxyphenyl)-propane-1,2-diol dimer (**CD-II** type condensation) (Fig. 3A, S3B, and S5A†). In the NLBTH-treated **GG** sample, the phenyl-dihydrobenzofuran type condensation products (*e.g.*, 4-(2-(hydroxymethyl)-7-methoxy-2,3-dihydrobenzofuran-3-yl)-2-methoxyphenol, a dimer from intramolecular condensation, **CD-III** type condensation) were the most abundant together with a small amount of **CD-I** type condensation products (Fig. 3B, S3A, and S5B†). This observation further established that the cleavage of the β-*O*-4-aryl ether bond was not the dominant reaction of **GG** in NLBTH. It was apparent that condensation mostly occurred *via* the α-benzyl carbocation by its electrophilic aromatic substitution on the electron-rich aromatic rings, forming a new C–C linkage, which resulted in characteristic correlation signals from the α-position of **CD-I**, **CD-II**, and **CD-III** type condensation products at δ_C/δ_H 50.8/4.18, 48.9/4.40, and 53.0/3.44 ppm, respectively. The identification of condensation products mentioned earlier brings new insight into the competition between the lignin depolymerization and condensation *via* the α-benzyl carbocation intermediate as catalyzed by both LiBr trihydrate and acid.

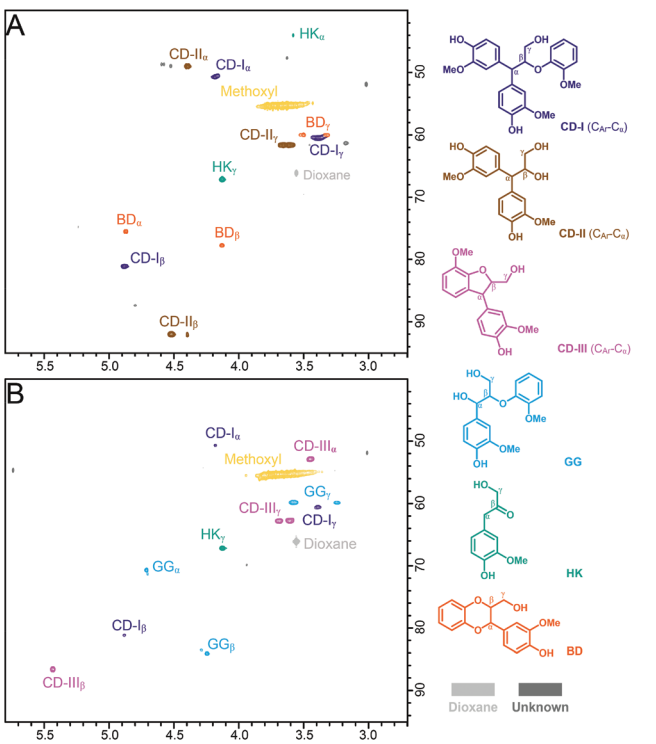

Fig. 3 HSQC NMR spectra of **GG** reaction products in the LiBr trihydrate reaction at 100 °C with 10 mM HCl for 10 min (A) and without acid (B) for 240 min.

3.3 Proposed mechanisms of lignin reactions in the LiBr trihydrate system

Based on the results and discussions mentioned above, pathways of lignin depolymerization to form **BD** and **HK** moieties and condensation reactions in the LiBr trihydrate system are proposed, as illustrated in Fig. 4 and S6.† In this system, the benzyl carbocation is logically the essential intermediate toward various products. There are two feasible routes to form the benzyl carbocation. Route I, which has been extensively elucidated in acidic systems, is initiated by acid-induced protonation of the benzyl alcohol and followed by dehydration to form the α-carbocation. Alternatively, in Route II, LiBr is postulated to catalyze the slow formation of the benzyl carbocation *via* reversible substitution of the α-hydroxyl by the bromide in the system. Route II is proposed based on the observation that condensation reactions occurred when **GG** was treated in NLBTH (LiBr alone without acid). In addition, Route II was

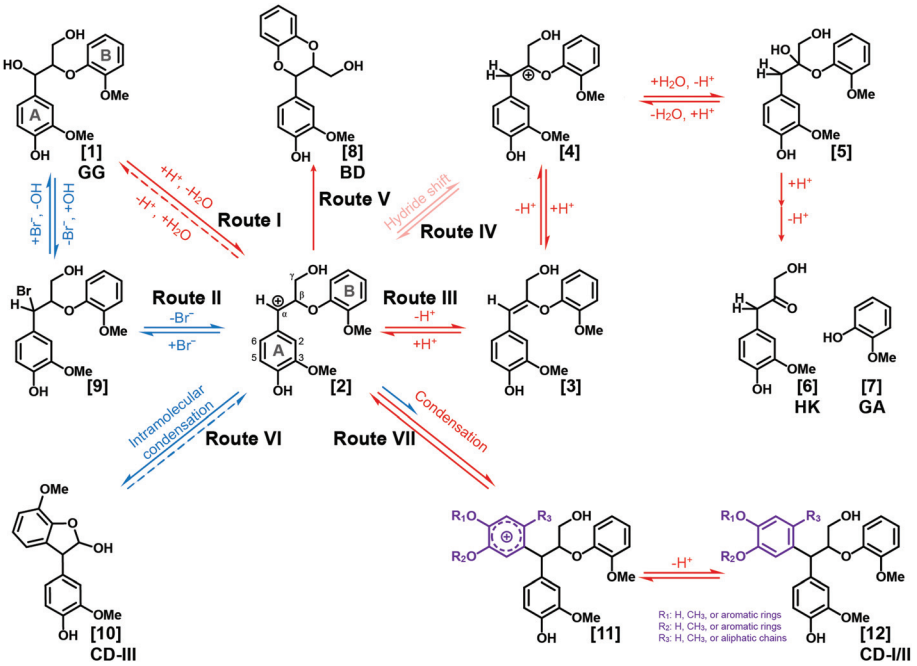

Fig. 4 Proposed lignin depolymerization and condensation mechanisms.

supported by the experiment in which 3,4,5-trimethoxylbenzyl alcohol (**TMBA**) was treated in the NLBTH system. As shown in Fig. S7A,† both the α-brominated intermediate of **TMBA** and its subsequent condensation product were detected, suggesting that LiBr alone did lead to the formation of the α-carbocation which then attacked the electron-rich 2/6-position on the aromatic ring of **TMBA**, resulting in the condensation products. The benzyl carbocation can then be subsequently transferred from the α- to the β-position either by the small equilibrium in Route III *via* an enol ether intermediate or in Route IV *via* direct hydride shift.[42] Following trapping of the β-carbocation by H_2O, cleavage of the β-*O*-4-aryl ether bond occurs, releasing the **HK** and **GA** moieties. As **GA** was barely detected in the absence of acids, both Routes III and IV were presumed to be exclusively acid-catalyzed processes.

The reactive benzyl carbocation intermediate can also lead to the formation of **BD** moieties *via* Route V, which is supported by the results mentioned above that the **BD** structures were identified in the products from both native lignins and **GG** in ALBTH. The nucleophilic methoxyl oxygen on the **GA** ring of **GG** can intramolecularly trap the benzyl carbocation, resulting in a **BD** moiety from β-*O*-4-aryl ethers after demethylation. It seems that trapping the benzyl carbocation by C3/5-methoxyl is the first step in **BD** formation followed by demethylation. Otherwise, other demethylation structures besides **BD** should have been identified from the GC-MS and NMR analyses. In addition, no **BD** moiety is detected in the NLBTH system, suggesting the essentiality of an acid to the **BD** formation. It is worth mentioning that the detection of the **BD** moiety has never been reported in the products from the acidolysis of lignin or LMCs. The conversion of β-*O*-4-aryl ethers to **BD** (an acid-tolerant structure) suggests the possibility of a new strategy for lignocellulosic biomass valorization in the ALBTH system, *i.e.*, hydrolyzing polysaccharides efficiently to their component sugars[26,28] and converting all lignin β-ethers to benzodioxanes in an isolated lignin that is then converted to catechol-type monomers by hydrogenolysis.[38]

Based on the identified condensation products from the **GG** studies above, two condensation routes are proposed. In Route VI (Fig. 4), intramolecular condensation occurs *via* electrophilic aromatic substitution by the benzyl carbocation on the electron-rich C5-carbon on the **B**-ring. The resultant phenyldihydrobenzofuran structure (**CD-III**) was detected only in the NLBTH system, the analog of which was also reported in the previous model compound study using 1-phenyl-2-phenoxy-1,3-propanediol (**PD**) and 1-(4-hydroxyphenyl)-2-phenoxy-1,3-propanediol (**HH**) in dilute H_2SO_4.[40,44,49] However, the **CD-III** structures were not detected from **GG** dimers under acidic conditions in several LMC studies including our own. The observation in this study suggested that the presence of acid might greatly inhibit the intramolecular condensation of **GG** from occurring in the LiBr trihydrate system, possibly due to the overwhelming prevalence of intermolecular condensation. As proposed in Route VII, the benzyl carbocation readily attacks the electron rich carbon on the aromatic rings. The reactive sites on the ring may vary depending on the ring substituents. For example, the favorable sites are the C1 position (*para* to the hydroxyl substituent) for **GA** (R_1: H, R_2: CH_3, and R_3: H) and the C6 position (*para* to the methoxyl substituent) for lignin units (R_1: H, R_2: CH_3, and R_3: aliphatic side chain) shown in Fig. 4. Three factors may affect the regioselectivity of the electrophilic substitution (condensation) of the aro-

matic rings: (1) the electron donating substituents activate the aromatic rings mostly at their *para* and *ortho* positions and their activation power follows the order OH > OMe > methyl ≈ side chain of lignin; (2) the substituents that form extra resonance structures with the aromatic rings favor *ortho*/*para* substitution; and (3) larger substituents (*e.g.*, aliphatic side chains) sterically inhibit the substitution at their *ortho* positions.

In analogy with traditional acid-catalyzed lignin depolymerization,[50,51] the trapping of a benzyl carbocation by the aromatic rings is considered to be the major condensation reaction in the ALBTH system. Each of the aromatic rings of **GG**, even after condensation, has active electron-rich sites, which are able to condense with a new benzyl carbocation to form C–C linkages. As a result, the intermolecular condensation reactions could generate high molecular weight products, such as those detected in the GPC analysis (Fig. S4†).

In order to further probe the condensation reactions occurring in ALBTH, **TMBA** (a benzyl carbocation generator) was reacted with **GA** and creosol (**CS**), and the products were analyzed with GC-MS, as shown in Fig. S7B and S7C.† The results confirmed the proposed Route VII (Fig. 4) in which the C–C condensation mostly occurred between the benzyl carbocation and electron-rich aromatic rings. Creosol (**CS**) is a monomeric lignin-mimic without the carbocation-forming ability that, alone, was stable in ALBTH and NLBTH (~98% recoverable at 100 °C). When **CS** was introduced into the **GG** system in LiBr trihydrate, **CS** was significantly consumed, indicating that **CS** reacted with **GG** (Fig. 5). In the ALBTH system (Fig. 5A), the maximum yield of **GA** decreased significantly from 31.4 to 10.7% when **CS** was added, indicating that the addition of **CS** inhibited the cleavage of the β-*O*-4-aryl ether bond in **GG** that would generate **GA**. This is because, under the acidic condition, the protonation of the benzyl alcohol of **GG** readily occurs and yields the benzyl carbocation, and its trapping by the excess creosol in the system forms the C_α–C_{aryl} linkage, which apparently blocks the pathway for cleavage of the β-*O*-4-aryl ether linkage *via* the analog of Route III or IV. In NLBTH (Fig. 5B), the **GG** consumption was much slower than that in ALBTH, as only LiBr contributed to the formation of the benzyl carbocation. In this case, the presence of **CS** produced no significant changes to **GG** consumption, indicating that the rate-limiting step of the condensation reactions in NLBTH is formation of the benzyl carbocation.

To summarize the findings of the mechanistic studies using LMCs, both LiBr and acid can induce the formation of the benzyl carbocation intermediate, which is crucial to lignin depolymerization and **BD** formation. Although LiBr exerts synergistic effects on the formation of the benzyl carbocation, the acid dominates the catalysis of both the formation of the benzyl carbocation and the subsequent cleavage of the β-*O*-4-aryl ether bonds to yield **HK** and demethylation to yield **BD** moieties. The undesirable competing pathway is the formation of C–C bonds between the benzyl carbocation and the electron-rich aromatic rings, which is catalyzed by both LiBr and acid.

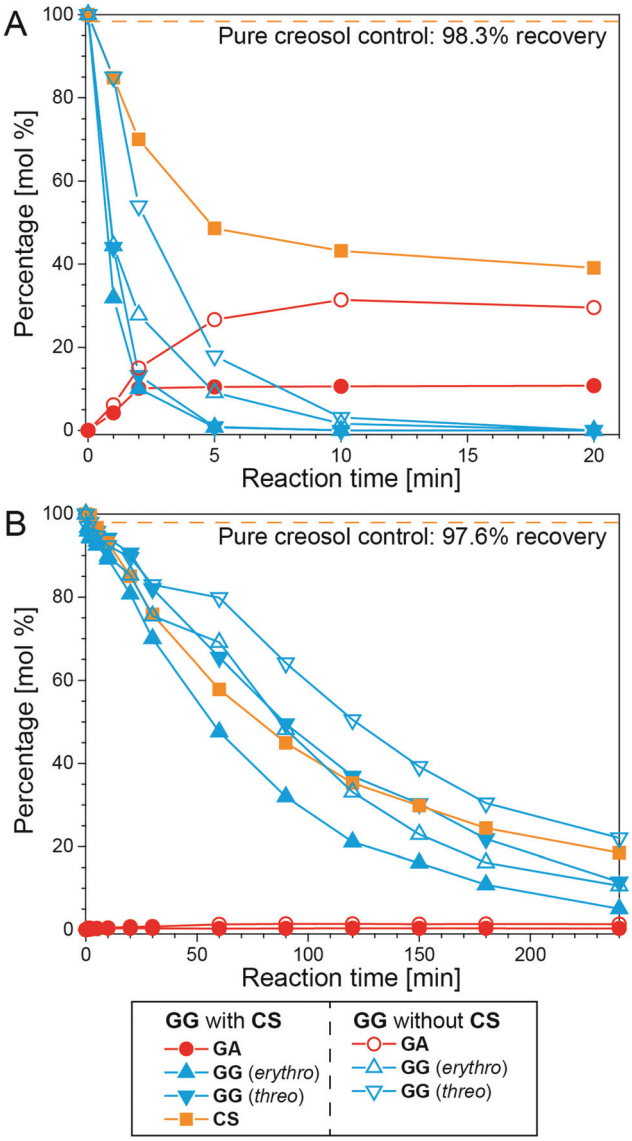

Fig. 5 The reaction of **GG** with **CS** in ALBTH with 10 mM HCl (A) and NLBTH (B). Reaction conditions: 100 °C, **GG** to **CS** ratio: 1/1 (w/w); no addition of **CS** as the control.

3.4 Suppressed lignin condensation in the ALBTH system

In any process of lignin isolation and depolymerization for downstream valorization, condensation is intrinsically undesirable. Although the LMC studies above demonstrated the possible condensation reactions occurring in ALBTH and NLBTH systems, the condensation products (containing C_α–C_{aryl} bonds), interestingly, remained at a minimal level in the real ALBTH lignins. In the HSQC NMR spectra (Fig. 1B, D, F, and H), the $^1H/^{13}C$ correlation signals at δ_C/δ_H (45–52)/(4.0–5.0) ppm from the assignment of the condensation structures at the C_α position were negligible. This observation indicated that the C–C condensation between the α-carbocation and an aromatic carbon was greatly suppressed during the ALBTH treatment of lignocellulosic biomass. The conden-

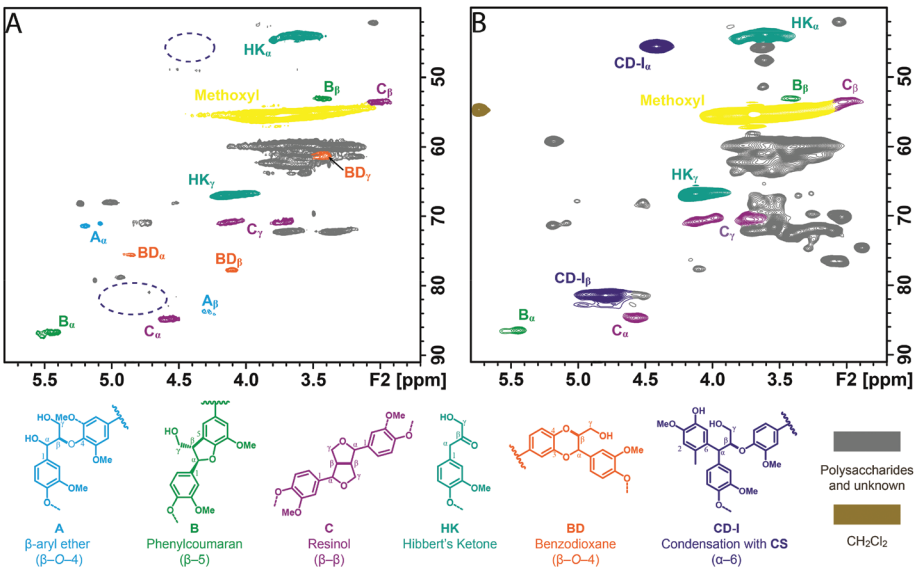

Fig. 6 Evaluation of condensation in ALBTH lignin from Douglas fir without creosol (A) and with addition of creosol (B, 5.5/1, w/w) at 110 °C.

sation disparity between the real lignin and LMCs might result from their solubility, status, and mobility in ALBTH (*i.e.*, the accessibility of electron-rich aromatics to the benzyl carbocation). In the case of the LMC reactions, the small aromatic molecules are either well dispersed or are dissolved in the system. Once the benzyl carbocation is formed, the nearby electron-rich (nucleophilic) aromatic carbons can readily succumb to attack by the carbocation, resulting in the C_α–C_{aryl} condensation products. On the other hand, lignin and lignin moieties are insoluble and tend to coil and aggregate as large particles in the ALBTH medium. The benzyl carbocation and the electron-rich aromatic rings from larger lignin polymers are therefore less mobile and have fewer chances to react with each other because of the steric and physical hindrance. Instead, the intramolecular cleavage of β-*O*-4-aryl ether bonds and the formation of **BD** from the benzyl carbocation are promoted. As a result, the ALBTH lignin has abundant uncondensed moieties (**HK** and **BD**) with limited condensation structures, which is consistent with our findings that the ALBTH lignin has low molecular weight and good solubility in many organic solvents.

In order to verify the hypothesis that condensation is unfavorable in real lignin due to limited mobility and accessibility, the lignocellulosic biomass (*e.g.*, Douglas fir) was treated in ALBTH in the presence of a monomeric lignin model nucleophile (**CS**). As expected, the resultant lignin featured significant correlation signals at δ_C/δ_H 45.4/4.41 ppm (α-position) and 81.4/4.80 ppm (β-position) due to condensation with **CS** (Fig. 6B), whereas the lignin without **CS** had negligible signals corresponding to condensation structures (Fig. 6A, the same as Fig. 1E). The results indicated that **CS**, as a small and mobile nucleophile, condensed readily with the lignin benzyl carbocation and formed C_α–C_{aryl} bonds; in contrast the condensation between two real lignin polymers was limited. These observations confirmed that the aromatic carbons and the benzyl carbocation in the solid-state lignin are less accessible to each other, contributing to the limited condensation reactions in ALBTH.

To demonstrate whether the uncondensed nature of the ALBTH lignin benefits its downstream valorization, preliminary hydrogenolysis of the ALBTH lignin from poplar was conducted using a Pd/C catalyst in methanol under 40 bar H_2 at 220 °C for 6 h. For comparison, Klason lignin (representing a condensed lignin) from poplar and native lignin from poplar were also hydrogenolyzed under the same conditions. As shown in Table S2,† over 96.0% of the ALBTH lignin was converted to a methanol-soluble lignin oil. Under the same conditions, only 29.6% of the Klason lignin was converted into the oil, whereas 63.7% was retained as an insoluble residue. On the other hand, 93.1% of the native lignin in poplar was hydrogenolyzed to an oil. These observations suggested that the ALBTH lignin had a comparable response to hydrogenolysis as with the native lignin, and was much better than the Klason lignin. These preliminary results verified that the ALBTH lignin may be a good lignin feedstock for downstream valorization, *via* hydrogenolysis, for example.

4. Conclusions

In this study, we illustrated how the treatment of lignocellulose in the ALBTH system achieved depolymerization and separation of lignin in its solid state without dissolution after nearly quantitative hydrolysis of polysaccharides to sugars. A pure lignin could be isolated from various woody and grass biomass sources, also essentially quantitatively. The lignin was extensively depolymerized with a minimal level of condensation. The most vulnerable β-*O*-4-aryl ether bonds were selec-

tively cleaved/transformed to uncondensed **HK** and **BD** moieties. Notably, **BD** was identified and confirmed for the first time in an acid-depolymerized lignin; its appearance suggests the possibility of using simpler routes toward catechol-type monomers that may be attractive for lignin valorization.

Model compound studies using **GG** revealed that the formation of the benzyl carbocation is the prerequisite for both depolymerization and condensation. LiBr and HCl in the ALBTH system synergistically catalyze the formation of the benzyl carbocation, which subsequently leads to either an **HK** moiety *via* the cleavage of the β-*O*-4-aryl ether bond or a **BD** moiety *via* the demethylation of methoxyls on the aromatic rings. The benzyl carbocation may also attack the electron-rich aromatic rings of lignin, resulting in undesirable condensation products. However, we found that the level of condensation (formation of C_α–C_{aryl} bonds) in real ALBTH lignin was surprisingly low. It was postulated that solid-state lignin reactions in ALBTH suppressed the condensation due to the reduced mobility and accessibility of the rigid lignin moieties (benzyl carbocations and electron-rich aromatic carbons) to each other. These findings together with preliminary hydrogenolysis results suggested that the ALBTH method may provide a new strategy to separate a useful, less condensed lignin from biomass for downstream valorization.

Author contributions

XP initiated the study. NL and XP designed the experiments and completed most of the data analyses and writing. NL conducted most of the lab work. YL, JR, CY, XY, and XL contributed to the data analyses and discussions. CY also made contributions to the whole-cell-wall NMR experiments. YL performed the GC-MS analysis of the **GG** reaction products, and YL and JR contributed to the interpretation and assignment of some NMR data, in particular the confirmation of the **BD** structure. All authors were involved in writing or proofing the manuscript.

Conflicts of interest

There are no conflicts of interest to declare.

Acknowledgements

The financial support from the National Science Foundation (NSF) (CBET 1159561), the U.S. Department of Agricultural (USDA) National Institute of Food and Agriculture, and the McIntire Stennis project (1006576) are acknowledged. Dr Gaojin Lyu kindly provided the β-ether lignin model compound used in this study. The NMR analysis was conducted in the Magnetic Resonance Facility in the Chemistry Department at the University of Wisconsin–Madison. Ning Li would like to thank the China Scholarship Council (CSC) for partially supporting his PhD study at the University of Wisconsin–Madison. Yanding Li and John Ralph were funded by the DOE Great Lakes Bioenergy Research Center (DOE BER Office of Science DE-SC0018409).

References

1 B. M. Upton and A. M. Kasko, *Chem. Rev.*, 2015, **116**, 2275–2306.
2 N. Mahmood, Z. Yuan, J. Schmidt and C. C. Xu, *Renewable Sustainable Energy Rev.*, 2016, **60**, 317–329.
3 R. Rinaldi, R. Jastrzebski, M. T. Clough, J. Ralph, M. Kennema, P. C. Bruijnincx and B. M. Weckhuysen, *Angew. Chem., Int. Ed.*, 2016, **55**, 8164–8215.
4 C. Xu, R. A. D. Arancon, J. Labidi and R. Luque, *Chem. Soc. Rev.*, 2014, **43**, 7485–7500.
5 Z. Sun, B. L. Fridrich, A. de Santi, S. Elangovan and K. Barta, *Chem. Rev.*, 2018, **118**, 614–678.
6 G. F. De Gregorio, C. C. Weber, J. Gräsvik, T. Welton, A. Brandt and J. P. Hallett, *Green Chem.*, 2016, **18**, 5456–5465.
7 B. J. Cox and J. G. Ekerdt, *Bioresour. Technol.*, 2012, **118**, 584–588.
8 B. J. Cox, S. Jia, Z. C. Zhang and J. G. Ekerdt, *Polym. Degrad. Stab.*, 2011, **96**, 426–431.
9 J. S. Luterbacher, A. Azarpira, A. H. Motagamwala, F. Lu, J. Ralph and J. A. Dumesic, *Energy Environ. Sci.*, 2015, **8**, 2657–2663.
10 P. J. Deuss, M. Scott, F. Tran, N. J. Westwood, J. G. de Vries and K. Barta, *J. Am. Chem. Soc.*, 2015, **137**, 7456–7467.
11 C. W. Lahive, P. J. Deuss, C. S. Lancefield, Z. Sun, D. B. Cordes, C. M. Young, F. Tran, A. M. Slawin, J. G. de Vries, P. C. Kamer, N. J. Westwood and K. Barta, *J. Am. Chem. Soc.*, 2016, **138**, 8900–8911.
12 L. Shuai, M. T. Amiri, Y. M. Questell-Santiago, F. Heroguel, Y. Li, H. Kim, R. Meilan, C. Chapple, J. Ralph and J. S. Luterbacher, *Science*, 2016, **354**, 329–333.
13 D. M. Miles-Barrett, A. R. Neal, C. Hand, J. R. Montgomery, I. Panovic, O. S. Ojo, C. S. Lancefield, D. B. Cordes, A. M. Slawin, T. Lebl and N. J. Westwood, *Org. Biomol. Chem.*, 2016, **14**, 10023–10030.
14 T. Yokoyama, *J. Wood Chem. Technol.*, 2014, **35**, 27–42.
15 P. J. Deuss, C. S. Lancefield, A. Narani, J. G. de Vries, N. J. Westwood and K. Barta, *Green Chem.*, 2017, **19**, 2774–2782.
16 S. Aziz and K. Sarkanen, *Tappi J.*, 1989, **72**, 169–175.
17 X. Pan, C. Arato, N. Gilkes, D. Gregg, W. Mabee, K. Pye, Z. Xiao, X. Zhang and J. Saddler, *Biotechnol. Bioeng.*, 2005, **90**, 473–481.
18 A. Rahimi, A. Ulbrich, J. J. Coon and S. S. Stahl, *Nature*, 2014, **515**, 249–252.
19 H. Nimz and R. Casten, *Eur. J. Wood Wood Prod.*, 1986, **44**, 207–212.
20 X.-J. Pan and Y. Sano, *Holzforschung*, 1999, **53**, 590–596.
21 J. Li, G. Henriksson and G. Gellerstedt, *Bioresour. Technol.*, 2007, **98**, 3061–3068.

22 M. Funaoka, T. Kako and I. Abe, *Wood Sci. Technol.*, 1990, **24**, 277–288.
23 K. Shimada, S. Hosoya and T. Ikeda, *J. Wood Chem. Technol.*, 1997, **17**, 57–72.
24 T. Imai, T. Yokoyama and Y. Matsumoto, *J. Wood Sci.*, 2011, **57**, 219–225.
25 W. Lan, M. Talebi Amiri, C. M. Hunston and J. Luterbacher, *Angew. Chem., Int. Ed.*, 2017, **130**, 1–6.
26 X. Pan and L. Shuai, *US* 9187790B2, 2015.
27 L. Shuai, Ph.D. Thesis, University of Wisconsin-Madison, 2012.
28 N. Li, X. Pan and J. Alexander, *Green Chem.*, 2016, **18**, 5367–5376.
29 X. Yang, N. Li, X. Lin, X. Pan and Y. Zhou, *J. Agric. Food Chem.*, 2016, **64**, 8379–8387.
30 Y. Liu, G. Lyu, X. Ji, G. Yang, J. Chen and L. A. Lucia, *BioResources*, 2016, **11**, 5816–5828.
31 J.-Y. Kim, E.-J. Shin, I.-Y. Eom, K. Won, Y. H. Kim, D. Choi, I.-G. Choi and J. W. Choi, *Bioresour. Technol.*, 2011, **102**, 9020–9025.
32 M. S. Jahan and S. P. Mun, *Bangladesh J. Sci. Ind. Res.*, 2010, **44**, 271–280.
33 A. Tolbert, H. Akinosho, R. Khunsupat, A. K. Naskar and A. J. Ragauskas, *Biofuels, Bioprod. Biorefin.*, 2014, **8**, 836–856.
34 L. Zoia, A. W. King and D. S. Argyropoulos, *J. Agric. Food Chem.*, 2011, **59**, 829–838.
35 C. Heitner, D. Dimmel and J. Schmidt, *Lignin and lignans: Advances in chemistry*, CRC press, 2016.
36 S. D. Mansfield, H. Kim, F. Lu and J. Ralph, *Nat. Protoc.*, 2012, **7**, 1579–1589.
37 F. Chen, Y. Tobimatsu, D. Havkin-Frenkel, R. A. Dixon and J. Ralph, *Proc. Natl. Acad. Sci. U. S. A.*, 2012, **109**, 1772–1777.
38 Y. Li, L. Shuai, H. Kim, A. H. Motagamwala, J. K. Mobley, F. Yue, Y. Tobimatsu, D. Havkin-Frenkel, F. Chen, R. A. Dixon, J. S. Luterbacher, J. A. Dumesic and J. Ralph, *Sci. Adv.*, 2018, submitted.
39 K. Barta, G. R. Warner, E. S. Beach and P. T. Anastas, *Green Chem.*, 2014, **16**, 191–196.
40 M. R. Sturgeon, S. Kim, K. Lawrence, R. S. Paton, S. C. Chmely, M. Nimlos, T. D. Foust and G. T. Beckham, *ACS Sustainable Chem. Eng.*, 2013, **2**, 472–485.
41 G. Wang and H. Chen, *Sep. Purif. Technol.*, 2016, **157**, 93–101.
42 H. Ito, T. Imai, K. Lundquist, T. Yokoyama and Y. Matsumoto, *J. Wood Chem. Technol.*, 2011, **31**, 172–182.
43 L. H. Hoo, K. V. Sarkanen and C. D. Anderson, *J. Wood Chem. Technol.*, 1983, **3**, 223–243.
44 S. Yasuda and K. Ota, *Holzforschung*, 1987, **41**, 59–65.
45 T. Imai, T. Yokoyama and Y. Matsumoto, *J. Wood Chem. Technol.*, 2012, **32**, 165–174.
46 J. R. Obst, *Holzforschung*, 1983, **37**, 23–28.
47 S. Sadula, O. Oesterling, A. Nardone, B. Dinkelacker and B. Saha, *Green Chem.*, 2017, **19**, 3888–3898.
48 C. G. Yoo, S. Zhang and X. Pan, *RSC Adv.*, 2017, **7**, 300–308.
49 C. Zhang, H. Li, J. Lu, X. Zhang, K. E. MacArthur, M. Heggen and F. Wang, *ACS Catal.*, 2017, **7**, 3419–3429.
50 C. Li, X. Zhao, A. Wang, G. W. Huber and T. Zhang, *Chem. Rev.*, 2015, **115**, 11559–11624.
51 L. Shuai and B. Saha, *Greem Chem.*, 2017, **19**, 3752–3758.